JOURNAL OF SOLID STATE CHEMISTRY 69, 202–214 (1987)

Two New Trigonal Magnesium Heteropolytungstates: Crystal Structures, Topotactic Relations, and Thermal Dehydration

JOHN R. GÜNTER* AND WOLFGANG BENSCH

Institute for Inorganic Chemistry, University of Zürich, Winterthurerstrasse 190, CH-8057 Zürich, Switzerland

Received June 16, 1986; in revised form November 3, 1986

Trigonal $Mg_8SiW_9O_{37} \cdot 24.5H_2O$ has been crystallized and its thermal dehydration studied. Its crystal structure (space group $P31c$, $a = 13.510(1)$, $c = 15.554(2)$ Å, $Z = 2$) contains two different complex units, one of which is a group of four edge-sharing MgO_6 octahedra, whereas the other contains the same arrangement as a base, onto which three groups of three edge-sharing WO_6 octahedra each are arranged so as to share corners with each other and with the base. This unit surrounds a tetrahedral interstice occupied by silicon. On heating, interstitial water is lost first, and then another trigonal heteropolytungstate of composition $Mg_8SiW_9O_{37} \cdot 12H_2O$ is formed (space group $P31c$, $a = 13.516(4)$, $c = 13.874(1)$ Å, $Z = 2$), differing from its parent compound by displacement of some magnesium atoms in such a way as to connect all the larger complex units, the smaller ones being destroyed. The displaced magnesium is now in an unusual fivefold coordination. Dehydration up to this point is highly topotactic and reversible. On further heating, the remaining water is lost and the lattice collapses into an amorphous state, which at higher temperatures crystallizes into a phase similar to high-temperature $MgWO_4$ and then transforms into the stable wolframite structure of $MgWO_4$.

Introduction

Experiments aimed at reproducing the preparation of a phase described as cubic $MgWO_4$ (*1*) led to the crystallization of three distinctly different products: rhombic dodecahedra of the cubic phase, consequently found to consist of a new type of heteropolytungstate (*2*), strongly aggregated platelets of $MgWO_4 \cdot 2H_2O$ (*3*), and needles with a hexagonal cross section. None of these phases corresponds to any of the compounds which are described in the literature about the system $Mg/W/O/H_2O$, compiled in (*3*). The present paper deals with the preparation and thermal dehydration behavior of the needle-shaped crystals, as well as with the results of single-crystal X-ray diffraction structure determinations of these and one of their dehydration products.

Experimental

Equal volumes of 1 *M* solutions of magnesium chloride and of sodium tungstate were mixed at room temperature, sealed in Pyrex tubes filled to 90–95%, and stored at 90°C for one to several weeks. The glass walls were then found to be covered with a white layer of crystals, from which the hexagonal needles were isolated mechanically under a binocular. Their thermal dehydration was followed by thermogravimetry and

* Author to whom correspondence should be addressed.

0022-4596/87 $3.00

differential thermal analysis (Mettler TA 2000C and Perkin–Elmer TGS-2), as well as by continuous high-temperature X-ray powder diffraction (Guinier–Lenné camera, Nonius Delft NL, Cu$K\alpha$ radiation). Scanning electron micrographs were recorded by means of a microscope Stereoscan S-4 (Cambridge Instruments) and the elemental composition was determined by energy-dispersive X-ray spectroscopy (EDAX). The latter showed the absence of all elements with $Z > 11$ except for Mg and W, with an approximate atomic ratio of 1 : 1 for these two metals. However, the crystal structure analysis suggested an incorporation of Si from the Pyrex tubes, and this element cannot be analyzed by energy-dispersive spectroscopy in the presence of W because of peak overlap. Therefore, additional analyses were performed by means of an electron beam microanalyzer (ARL) equipped with a wavelength-dispersive crystal spectrometer, and indeed showed the presence of more than trace amounts of Si. As the crystals dehydrated visibly (compare Fig. 4) within the vacuum of the instrument, the analytical results were compared with the formula derived from crystal structure analysis of the partly dehydrated compound B ($Mg_8SiW_9O_{37} \cdot 12H_2O$):

experimental: Mg, 7.1 wt%; Si, 1.0 wt%; W, 63.8 wt%; O (diff.), 28.1 wt% (average from 19 measurements);

calculated: Mg, 7.2 wt%; Si, 1.1 wt%; W, 61.6 wt%; O/H_2O, 30.1 wt%.

The water content was checked by thermal analysis, the experimental value being 15.5 wt% compared to 15.2 wt% calculated from the formula.

Crystal Structure Determination of $Mg_8SiW_9O_{37} \cdot 24.5H_2O$ (Compound A)

Preliminary Weissenberg and precession photographs of compound A suggested a hexagonal symmetry, but inspection of the upper-level precession photographs revealed a slight deviation from it. From extinction conditions $000l$, $l = 2n$ and $hh2hl$, $l = 2n$ only, space groups $P31c$ and $P\bar{3}1c$ were possible. A white, needle-shaped crystal with hexagonal cross section (dimensions 0.035 × 0.035 × 0.15 mm) was mounted on an Enraf Nonius CAD4 single-crystal diffractometer with its crystallographic c-axis parallel to the Φ-axis of the diffractometer. Monochromatic MoK_α radiation (λ = 0.7107 Å) was used. The lattice parameters were refined with 25 automatically centered reflections (range $12.6 < \Theta < 16.8°$) to a = 13.510(1), c = 15.554(2) Å, V = 2458 Å^3. Out to $\Theta = 30°$ a total of 10,496 reflections were recorded using the $\omega - 2\Theta$-scan technique with Miller indices running from −19 to 19 for h, −3 to 19 for k, and −3 to 21 for l. Five orientation control reflections were remeasured every 250 recorded data and the stability of the intensity was checked by 5 reflections every 10,000 sec of measuring time. No decay was detectable. To diminish the bias, which is introduced if the reflections with negative intensities are omitted, all data with intensity lower than $0.5\sigma(I)$ were processed as $0.25\sigma(I)$ and included in the data set. The averaging of the reflections led to 2941 unique data. Lorentz, polarization, and numerical absorption corrections (minimum transmission 0.500 and maximum transmission 0.569; R_{int} = 0.015 based on F_o) were applied. The structure was solved using the Patterson interpretation routine in SHELXS-84 (*4*) assuming the acentric space group $P31c$ and subsequent difference Fourier syntheses. In the final stages all metal atoms were refined anisotropically using 1581 unique data with $F > 5\sigma(F)$. At convergence $(\Delta/\sigma) \leq 0.006$. One oxygen atom was located with an unusually high isotropic temperature factor and with no bonds to metal atoms. The reason for this high-temperature factor may be the partial occupation of the sixfold position. Therefore, for the refinement of the site occupa-

tion factor the temperature factor of this atom was fixed at a value which corresponds to the mean isotropic temperature factor of the other oxygen atoms. The refined occupation factor was then 0.82, which is nearly equal to five O atoms, leading to a formula of $Mg_8SiW_9O_{37} \cdot 24.5H_2O$, with formula weight $M = 2910.2$, $\mu = 203.6$ cm^{-1}, and $Z = 2$. The weighting scheme $w = k/(\sigma^2(F) + 0.0003F^2)$ (k refined to 1.34) was based on intensity statistics and showed no dependence of the function minimized upon the magnitude of F_o or (sin Θ/λ). The final difference Fourier map exhibited as highest peak 3.5 $e^-/Å^3$ near the heavy atoms and -3.1 $e^-/Å^3$ as hole. Final R and wR were 0.051 and 0.039, respectively. The absolute configuration was determined by reversing the signs of the coordinates of all atoms. The wR obtained in that way was 0.051, which is significantly higher than the wR for the configuration chosen for the structure determination. This conclusion was supported by applying the Hamilton test (*5*).

Crystal Structure of Compound A

The atomic coordinates and thermal parameters, as well as the bond distances and angles, are summarized in Tables I and II, respectively. The relatively high standard deviations may be due to the lack of a good absorption correction. A projection of the structure along [001] is displayed in Fig. 1. The two distinctly different isolated complex building units may be described as follows: one (unit (1)) consists of four edge-sharing MgO_6 octahedra containing Mg(2) and Mg(3) atoms. The Mg–O distances range from 2.05(3) to 2.15(3) Å for Mg(2) and from 2.08(3) to 2.10(3) Å for Mg(3). These Mg–O distances are normal and are observed in many MgO_6 octahedra-containing compounds (*3, 6*). The O–Mg–O angles indicate only a slight distortion from the ideal octahedral symmetry. The second comlex building unit (unit (2)) contains an arrangement similar to unit (1) with $Mg(1)O_6$ and $Mg(4)O_6$ octahedra as base, onto which three groups of three edge-sharing W coordination octahedra each are arranged so as to share corners with each other and the base. This unit surrounds a tetrahedral interstice occupied by Si.

If the metal atoms in the octahedra of this

TABLE I

POSITIONAL COORDINATES AND THERMAL PARAMETERS FOR $Mg_8SiW_9O_{37} \cdot 24.5H_2O$ (COMPOUND A)[a]

Atom	x/a	y/b	z/c	U_{eq}
W(1)	0.6536(1)	0.5849(1)	0.0050	0.012(2)
W(2)	0.9109(2)	0.6061(2)	0.0039(2)	0.010(2)
W(3)	0.2301(2)	0.4831(2)	0.3237(2)	0.012(2)
Mg(1)	0.5821(10)	0.3992(11)	0.1910(10)	0.015(11)
Mg(2)	0.9202(10)	0.8467(8)	0.2780(9)	0.009(10)
Mg(3)	0.0000	0.0000	0.4406(15)	0.008(15)
Mg(4)	0.3333	0.6667	0.8542(18)	0.020(18)
Si	0.3333	0.6667	0.5137(19)	0.004(14)
O(1)	0.624(2)	0.692(2)	0.005(2)	0.019(6)
O(2)	1.046(2)	0.727(2)	0.004(2)	0.017(6)
O(3)	0.819(2)	0.677(3)	0.013(3)	0.019(6)
O(4)	0.947(2)	0.489(2)	−0.027(2)	0.012(5)
O(5)	0.082(2)	0.400(2)	0.373(2)	0.019(6)
O(6)	0.890(2)	0.565(2)	0.116(2)	0.022(7)
O(7)	1.067(2)	0.931(2)	0.353(2)	0.010(5)
O(8)	0.637(2)	0.542(2)	0.114(2)	0.018(6)
O(9)	0.467(2)	0.723(2)	0.766(2)	0.020(6)
O(10)	0.392(2)	0.596(2)	0.313(2)	0.005(5)
O(11)	0.837(2)	0.695(2)	0.356(2)	0.023(7)
O(12)	0.199(2)	0.427(2)	0.220(2)	0.024(6)
O(13)	0.276(2)	0.386(2)	0.375(2)	0.021(6)
O(14)	0.988(3)	0.762(3)	0.211(2)	0.032(8)
O(15)	0.427(2)	0.806(2)	0.937(2)	0.028(7)
O(16)	0.500(2)	0.460(3)	0.283(2)	0.026(7)
O(17)	0.777(3)	0.759(3)	0.199(2)	0.033(8)
O(18)	0.910(2)	0.862(2)	0.523(2)	0.021(7)
O(19)	0.259(2)	0.537(2)	0.475(2)	0.013(5)
O(20)	1.000	1.000	0.211(4)	0.033(14)
O(21)	0.333	0.667	0.609(4)	0.032(13)
O(22)	0.430(3)	0.835(3)	0.111(3)	0.032

Atom	U_{11}	U_{22}	U_{33}	U_{23}	U_{13}	U_{12}
W(1)	0.012(1)	0.009(1)	0.015(1)	0.002(1)	0.000(1)	0.007(1)
W(2)	0.007(1)	0.008(1)	0.016(1)	0.000(1)	0.000(1)	0.002(1)
W(3)	0.014(1)	0.011(1)	0.011(1)	−0.003(1)	−0.001(1)	0.005(1)
Mg(1)	0.009(5)	0.023(7)	0.012(7)	−0.012(7)	−0.001(6)	0.010(5)
Mg(2)	0.009(6)	0.007(6)	0.012(7)	−0.006(5)	−0.006(6)	0.001(5)
Mg(3)	0.007(6)	0.007(6)	0.010(12)	0.000	0.000	0.004(3)
Mg(4)	0.011(6)	0.011(6)	0.037(16)	0.000	0.000	0.006(3)
Si	0.002(5)	0.002(5)	0.008(12)	0.000	0.000	0.001(3)

[a] Standard deviations in the last significant digits are given in parentheses. The U_{eq} is defined as one third of the trace of the orthogonalized U tensor. For the oxygen atoms U_{eq} is equal to the isotropic temperature factor.

TABLE II

BOND DISTANCES (Å) AND ANGLES (°) IN $Mg_8SiW_9O_{37} \cdot 24.5H_2O$ (COMPOUND A)

W(1) –O(1)	1.68(3)	O(1) –W(1)–O(8)	104(1)	O(9) –Mg(1)–O(8)	95(1)
W(1) –O(8)	1.77(3)	O(1) –W(1)–O(4)	102(1)	O(9) –Mg(1)–O(9)	84(1)
W(1) –O(4)	1.89(3)	O(1) –W(1)–O(3)	98(1)	O(9) –Mg(1)–O(6)	178(1)
W(1) –O(3)	1.94(2)	O(1) –W(1)–O(5)	91(1)		
W(1) –O(5)	2.09(3)	O(1) –W(1)–O(19)	165(1)	O(9) –Mg(1)–O(21)	88(1)
W(1) –O(19)	2.31(2)	O(8) –W(1)–O(4)	93(1)	O(9) –Mg(1)–O(16)	89(1)
		O(8) –W(1)–O(3)	94(1)	O(8) –Mg(1)–O(9)	177(1)
W(2) –O(2)	1.74(2)	O(8) –W(1)–O(5)	165(1)	O(8) –Mg(1)–O(6)	87(1)
W(2) –O(6)	1.81(3)	O(8) –W(1)–O(19)	89(1)	O(8) –Mg(1)–O(21)	91(1)
W(2) –O(3)	1.92(3)	O(4) –W(1)–O(3)	157(1)	O(8) –Mg(1)–O(16)	93(1)
W(2) –O(4)	1.94(3)	O(4) –W(1)–O(5)	83(1)	O(9) –Mg(1)–O(6)	95(1)
W(2) –O(13)	2.03(3)	O(4) –W(1)–O(19)	84(1)	O(9) –Mg(1)–O(21)	86(1)
W(2) –O(19)	2.34(3)	O(3) –W(1)–O(5)	85(1)	O(9) –Mg(1)–O(16)	90(1)
		O(3) –W(1)–O(19)	74(1)	O(6) –Mg(1)–O(21)	93(1)
W(3) –O(12)	1.73(3)	O(5) –W(1)–O(19)	76(1)	O(6) –Mg(1)–O(16)	90(1)
W(3) –O(13)	1.89(3)			O(21)–Mg(1)–O(16)	175(1)
W(3) –O(5)	1.90(2)	O(2) –W(2)–O(6)	102(1)		
W(3) –O(10)	1.90(2)	O(2) –W(2)–O(3)	100(1)	O(7) –Mg(2)–O(14)	175(1)
W(3) –O(10)	1.95(2)	O(2) –W(2)–O(4)	101(1)	O(7) –Mg(2)–O(20)	83(1)
W(3) –O(19)	2.43(3)	O(2) –W(2)–O(13)	93(1)	O(7) –Mg(2)–O(17)	99(1)
		O(2) –W(2)–O(19)	166(1)	O(7) –Mg(2)–O(7)	85(1)
Mg(1)–O(9)	2.02(3)	O(6) –W(2)–O(3)	92(1)	O(7) –Mg(2)–O(11)	93(1)
Mg(1)–O(8)	2.07(3)	O(6) –W(2)–O(4)	93(1)	O(14)–Mg(2)–O(20)	99(1)
Mg(1)–O(9)	2.07(3)	O(6) –W(2)–O(13)	164(1)	O(14)–Mg(2)–O(7)	91(1)
Mg(1)–O(6)	2.08(3)	O(6) –W(2)–O(19)	90(1)	O(14)–Mg(2)–O(17)	86(1)
Mg(1)–O(21)	2.17(4)	O(3) –W(2)–O(4)	157(1)	O(14)–Mg(2)–O(11)	86(1)
Mg(1)–O(16)	2.21(4)	O(3) –W(2)–O(13)	85(1)	O(20)–Mg(2)–O(7)	82(1)
		O(3) –W(2)–O(19)	74(1)	O(20)–Mg(2)–O(17)	99(1)
		O(4) –W(2)–O(13)	84(1)	O(20)–Mg(2)–O(11)	175(2)
Mg(2)–O(7)	2.05(3)	O(4) –W(2)–O(19)	84(1)	O(7) –Mg(2)–O(17)	177(1)
Mg(2)–O(14)	2.06(4)	O(13)–W(2)–O(19)	74(1)	O(7) –Mg(2)–O(11)	96(1)
Mg(2)–O(20)	2.07(3)			O(17)–Mg(2)–O(11)	84(1)
Mg(2)–O(7)	2.08(2)	O(12)–W(3)–O(13)	101(1)		
Mg(2)–O(17)	2.09(3)	O(12)–W(3)–O(10)	101(1)	O(18)–Mg(3)–O(18)	86(1) 3×
Mg(2)–O(11)	2.15(3)	O(12)–W(3)–O(5)	99(1)	O(18)–Mg(3)–O(7)	172(1) 3×
		O(12)–W(3)–O(10)	101(1)	O(7) –Mg(3)–O(7)	101(1) 3×
Mg(3)–O(18)	2.08(3) 3×	O(12)–W(3)–O(19)	173(1)	O(18)–Mg(3)–O(7)	91(1) 3×
Mg(3)–O(7)	2.11(3) 3×	O(13)–W(3)–O(10)	158(1)	O(18)–Mg(3)–O(7)	82(1) 3×
		O(13)–W(3)–O(5)	92(1)		
Mg(4)–O(9)	2.09(3) 3×	O(13)–W(3)–O(10)	87(1)	O(9) –Mg(4)–O(9)	82(1) 3×
Mg(4)–O(15)	2.10(3) 3×	O(13)–W(3)–O(19)	75(1)	O(9) –Mg(4)–O(15)	93(1) 3×
		O(10)–W(3)–O(5)	87(1)	O(9) –Mg(4)–O(15)	99(1) 3×
Si –O(19)	1.64(2) 3×	O(10)–W(3)–O(10)	86(1)	O(9) –Mg(4)–O(15)	174(1) 3×
Si –O(21)	1.48(6)	O(10)–W(3)–O(19)	84(1)	O(15)–Mg(4)–O(15)	86(1) 3×
		O(5) –W(3)–O(10)	160(1)		
		O(5) –W(3)–O(19)	76(1)	O(21)–Si –O(19)	112(1) 3×
		O(10)–W(3)–O(19)	84(1)	O(19)–Si –O(19)	107(1) 3×

unit are considered to be all of the same kind, it may be described as a Keggin structure with one additional octahedron: the Keggin structure is based on a central XO_4 tetrahedron (here SiO_4) surrounded by twelve MO_6 octahedra arranged in four

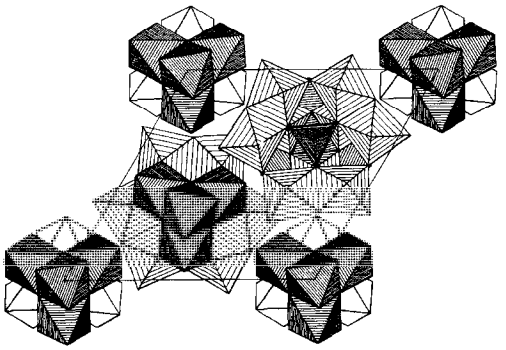

FIG. 1. Projection along [001] of the crystal structure of $Mg_8SiW_9O_{37} \cdot 24.5H_2O$ (compound A). Narrowly shaded: Mg coordination octahedra; widely shaded: W coordination octahedra; unshaded: Mg coordination octahedra on a different level. Interstitial water molecules not coordinated to metal atoms are omitted (*15*).

groups of three edge-sharing octahedra. These groups are linked by common corners with each other and with the central tetrahedron. The additional octahedron is connected to one of the threefold groups by three common edges.

All the WO_6 octahedra are of type (I) as defined by (*7*). In the W(1) and W(2) octahedra the metal atoms are clearly displaced from the centers towards the terminal oxygen atoms, thus forming one distinctly shorter bond. Additionally both types of tungsten atoms are surrounded by four bridging oxygen atoms with W–O distances ranging from 1.77(3) to 2.09(3) Å and one central oxygen atom (O(19)) with an elongated W–O bond length of 2.30(2) Å for W(1) and 2.34(3) Å for W(2). The environment of the third tungsten atom W(3) is more regular compared with that of W(1) and W(2). The $W(3)O_6$ octahedron is also of type (I) because the metal atom is displaced from the center towards the terminal O atom (W(3)–O(12): 1.73(3) Å). The distances between W(3) and the four bridging O atoms range from 1.89(3) to 1.95(2) Å. The octahedron around W(3) is completed by the central O atom O(19) with a bond length of 2.44(3) Å. Labelling the terminal oxygen atoms as O_A, the bridging O atoms as O_B, and the central O atoms as O_C we have calculated mean values $W–O_A = 1.72$, $W–O_B = 1.92$, and $W–O_C = 2.36$ Å. Bond length–bond strength correlations s of the form $s = (R_1/R)^N$, where s is Pauling's bond strength (bond valence), R is the metal–oxygen bond length, and R_1 and N are empirical parameters ($R_1 = 1.904$ Å and $N = 6.0$) (*16*), applied to $W–O_A$ lead to $s_{mean} = 1.84$. This value is smaller than the estimated s_{mean} for $W–O_A$ in the hexametalate ions $W_6O_{19}^{2-}$ (2.04) and larger than in Anderson structure anions like $(NiO_6W_6O_{18})^{8-}$ (1.5). The s_{mean} for $W–O_B$ and $W–O_C$ is 0.95 and 0.28, respectively, and thus about the same as calculated for $W_6O_{19}^{2-}$ (0.95 and 0.30) (*8*). The $O_A–W–O_B$ angles range from 91(1) to 104(1)° for W(1), from 93(1) to 102(1)° for W(2) and from 99(1) to 101(1)° for W(3). The $O_B–W–O_B$ angles between neighboring W–O bonds range from 83(1) to 94(1)° and those between W–O bonds extending on the opposite sides from a W atom range from 154(1) to 165(1)°. The W–W distances are between 3.398(1) and 3.411(1) Å and are typical for polytungstates (*9, 10*).

The Si–O distances are in the region found in other heteropolytungstates with one relatively short Si–O bond of 1.48 Å (*7*). Unfortunately, the oxygen atoms could not be refined anisotropically and therefore a libration correction could not be applied. Nevertheless, the O–Si–O angles deviate only a little from the ideal tetrahedral environment (see Table II).

The $Mg(1)O_6$ and $Mg(4)O_6$ octahedra are rather normal with Mg–O distances and O–Mg–O angles as observed in other MgO_6-containing compounds (*6*). The interstitial water molecules are situated between the two complex building units. The shortest distance between metal atoms and the oxygen atom O(22) is 3.66 Å. The shortest separations between oxygen atoms and the water molecule are in the range 2.73 to 3.13 Å.

Initial Steps of Thermal Dehydration

The thermogravimetric curve (Fig. 2) reveals a first weight loss of about 1.4% below 100°C. This step of the dehydration reaction is also observed on the heating X-ray powder diffraction diagram (Fig. 3) as a slight shortening of the *c*-axis dimension by ≈1.5%, the length of the other axes remaining unaffected. From the magnitude of the weight loss and the minimal change in unit cell dimensions, we conclude that this step of the reaction corresponds to the release of the interstitial water on the incompletely occupied crystallographic position. On further heating, more water is driven off between 100 and 210°C. The weight loss in this second step amounts to 9.9%. The high-temperature X-ray powder diffraction pattern shows this step to be associated with a much more pronounced shortening of the *c*-axis from 15.554 to 13.87 Å, whereas the other axes again remain essentially unaffected. The whole dehydration process up to this point is fully reversible and of an extremely high degree of topotaxy. This may be illustrated by the fact

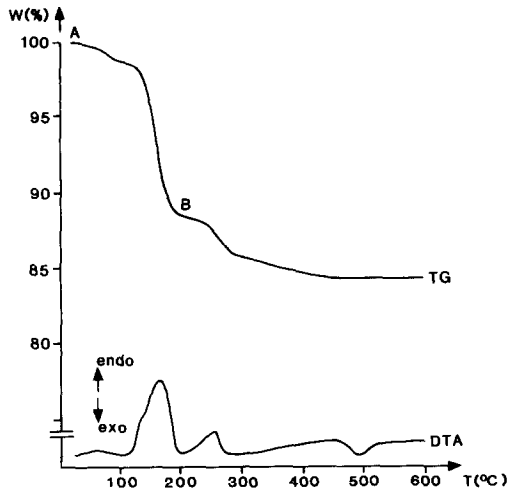

FIG. 2. Thermogravimetry and differential thermal analysis curves for $Mg_8SiW_9O_{37} \cdot 24.5H_2O$. Sample weight: 13.5 mg; atmosphere: flowing air; heating rate: 4°/min.

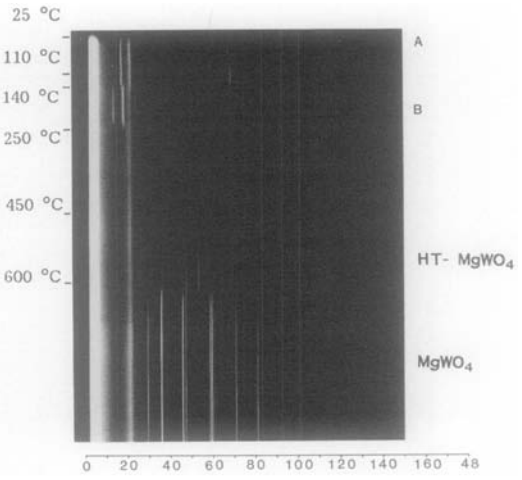

FIG. 3. Continuous high-temperature X-ray powder diffraction pattern of $Mg_8SiW_9O_{37} \cdot 24.5H_2O$ (Guinier–Lenné camera, CuK_α radiation).

that a single crystal of compound A, which has been oriented on the CAD4 diffractometer and the heated to 200°C, still yields sharp X-ray diffraction peaks, corresponding to the cell with reduced *c*, and after standing in air for 3 weeks again behaves largely as a single crystal, but has regained its original unit cell dimensions of compound A. The high degree of topotaxy is also evident from scanning electron micrographs (Fig. 4), which show the original needle-shaped crystals to contain strictly oriented cracks only perpendicular to the needle axis (*c*). This unusually high degree of perfect orientation of the product crystallites has made it possible to determine the crystal structure of the compound dehydrated to this stage by means of the four-circle diffractometer. This dehydrated pseudomorphous compound will consequently be named compound B. As the steps in the thermogravimetric curve are not clearly separated, the measured weight loss may not be used for an exact determination of the stoichiometry of compound B. Indeed, its crystal structure determination indicates a formula $Mg_8SiW_9O_{37} \cdot 12H_2O$, for which the second step of dehydration

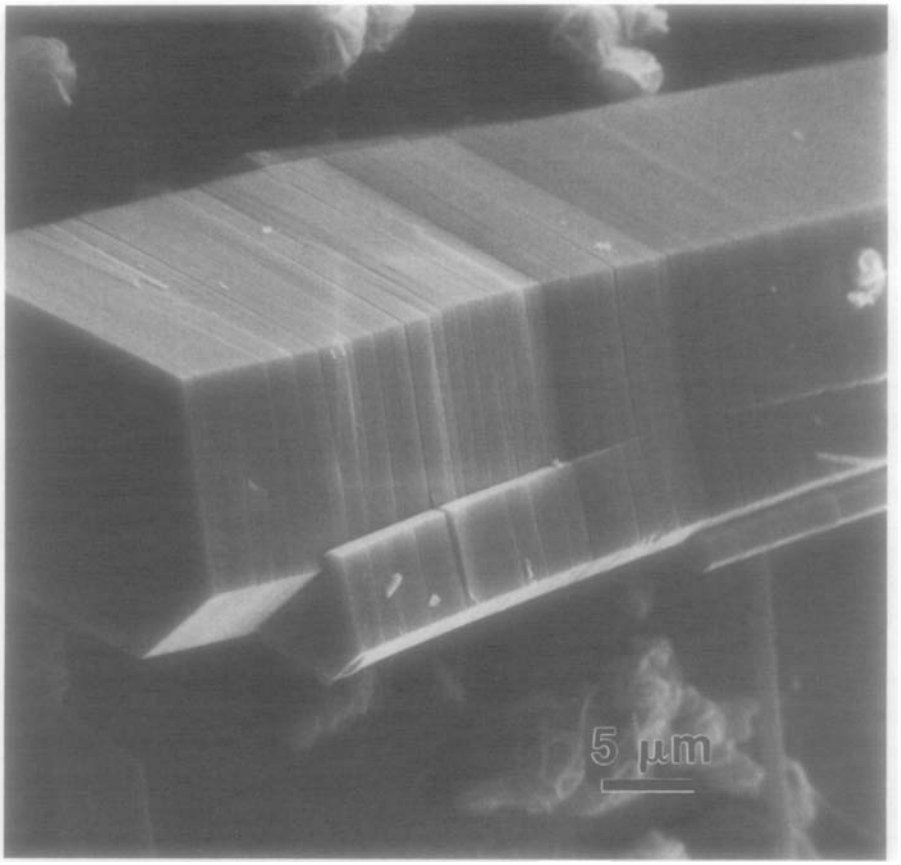

FIG. 4. Scanning electron micrograph of $Mg_8SiW_9O_{37} \cdot 24.5\ H_2O$ crystals dehydrated at 200°C to $Mg_8SiW_9O_{37} \cdot 12H_2O$ (compound B) pseudomorphs.

would correspond to a weight loss of only 8.0%.

Crystal Structure Determination of $Mg_8SiW_9O_{37} \cdot 12H_2O$ (Compound B)

Single crystals of compound A dehydrated isothermally at 200°C were investigated with the Weissenberg and precession film techniques to confirm their pseudo-single-crystal state and to determine their crystal system and space group. All crystals studied in this way showed a broadening of the reflections with high l indices and are more or less of poor quality. A few crystals even revealed weak diffuse reflections which contradict the extinction conditions of space group $P31c$. A crystal of the dehydrated compound with dimensions $0.06 \times 0.035 \times 0.165$ mm was mounted on a Syntex P21 diffractometer with the needle axis parallel to the Φ-axis of the diffractometer. The lattice parameters $a = 13.516(4)$, $c = 13.874(1)$ Å, and $V = 2195$ Å^3, as well as the orientation matrix, were determined using 16 reflections in the range $15 < \Theta < 22°$. A total of 7097 reflections were collected with the ω-scan technique (scan angle 3°, graphite monochromatized MoK_α radiation, $\lambda = 0.7107$ Å) up to $\Theta = 30°$ with Miller indices running from -19 to 19 for h, 0 to 19 for k, and 0 to 19 for l. Four orientation control reflections were remeasured every 150 data. The intensity was checked

by four reflections which were remeasured after 9000 sec of measuring time. Small anisotropic decay (≤8%); Lorentz, polarization, and numerical absorption corrections (minimum transmission 0.375 and maximum transmission 0.547; μ = 227 cm^{-1}; R_{int} = 0.02 based on F_o) were applied. For the structure determination, the atomic parameters of the tungsten atoms of compound A were used as starting parameters. All other atoms could be located by subsequent difference Fourier syntheses. In the final stages the metal atoms were refined anisotropically using 1585 unique data with $F > 6\sigma(F)$. At convergence $(\Delta/\sigma) \leq 0.07$. Final R and wR are 0.091 and 0.097, respectively. The weighting scheme $w = k/(\sigma^2(F) + 0.00026F^2)$ (k refined to 5.4) was based on intensity statistics and showed a small dependence of the function minimized upon the magnitude of F_o. The final difference Fourier map showed as highest peak 8.7 $e^-/Å^3$ and −6.6 $e^-/Å^3$ as hole. To determine the absolute configuration of the structure we have reversed the signs of the atomic coordinates. The wR value obtained was 0.097, which is exactly the same as for the configuration chosen for the refinement process. Therefore we could not decide whether we have chosen the correct configuration, but the similarities between the structures of compound A and compound B suggested that the decision was correct.

Both structures were refined with a full-matrix least-squares procedure using SHELX-76 (*11*). The scattering factors for the neutral atoms as well as the corrections for anomalous dispersion for both compounds were taken from (*12*).

Crystal Structure of Compound B

The atomic coordinates and thermal parameters are listed in Tables III and IV, respectively. The relatively high standard deviations are due to the poor quality of the measured pseudocrystal. A projection of the structure along [001] is drawn in Fig. 5. As mentioned above, compound B is a dehydrated product of compound A. The dehydration leads to a shortening of the c-axis by about 11%, whereas the lengths of the other two axes are almost not affected. The structure shows some features that are different from that of compound A. The complex building unit (1) formed by four edge-sharing MgO_6 octahedra in A is now destroyed. The Mg(2) atoms have moved in the direction of unit (2) and their octahedral environment is lost. Mg(2) is now surrounded by only five oxygen atoms. Its coordination polyhedron may be described as a distorted rectangular pyramid. This polyhedron is connected by common edges to the complex building unit (2) (see Table V), linking these units three-dimensionally by corner-sharing. The Mg–O distances in this unusual coordination polyhedron range from 1.98(8) to 2.21(7) Å and are rather normal for Mg–O bond distances. The O–Mg–O angles between neighboring oxygen atoms are between 80(2) and 95(2)°, whereas the other angles are between 118(3) and 147(3)°.

The $Mg(3)O_6$ octahedron remains essentially in the same position as in compound A and is nearly equally distorted compared with the $Mg(3)O_6$ octahedron in compound A, but now remains isolated.

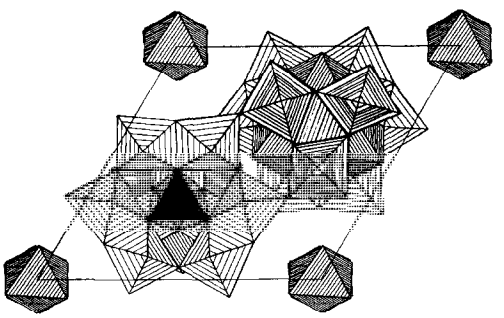

FIG. 5. Projection along [001] of the crystal structure of $Mg_8SiW_9O_{37} \cdot 12H_2O$ (compound B). Narrowly shaded: Mg coordination polyhedra; widely shaded: W coordination octahedra (*15*).

TABLE III

POSITIONAL COORDINATES AND THERMAL PARAMETERS FOR $Mg_8SiW_9O_{37} \cdot 12H_2O$ (COMPOUND B)[a]

Atom	x/a	y/b	z/c	U_{eq}
W(1)	0.6752(3)	0.5969(3)	0.0050	0.024(4)
W(2)	0.9228(3)	0.5979(3)	0.0051(3)	0.024(4)
W(3)	0.2419(3)	0.4837(2)	0.3021(3)	0.020(2)
Mg(1)	0.5871(19)	0.4111(20)	0.2125(14)	0.027(20)
Mg(2)	0.5203(19)	0.7593(22)	0.0503(17)	0.034(22)
Mg(3)	0.0000	0.0000	0.4620(24)	0.025(22)
Mg(4)	0.3333	0.6667	0.9037(27)	0.036(28)
Si	0.3333	0.6667	0.5055(56)	0.032(25)
O(1)	0.708(4)	0.646(4)	0.508(3)	0.011(8)
O(2)	0.069(5)	0.716(5)	0.013(5)	0.046(15)
O(3)	0.840(4)	0.687(3)	0.027(3)	0.007(7)
O(4)	0.949(3)	0.472(3)	0.986(3)	0.007(7)
O(5)	0.101(3)	0.396(4)	0.359(3)	0.019(9)
O(6)	0.902(4)	0.562(4)	0.138(4)	0.029(11)
O(7)	0.073(5)	0.927(5)	0.397(4)	0.036(11)
O(8)	0.663(4)	0.563(4)	0.137(3)	0.024(10)
O(9)	0.266(3)	0.733(3)	0.787(3)	0.014(8)
O(10)	0.393(3)	0.609(3)	0.301(3)	0.002(6)
O(12)	0.217(4)	0.431(4)	0.195(4)	0.035(11)
O(13)	0.293(4)	0.394(4)	0.364(4)	0.025(10)
O(15)	0.393(6)	0.797(4)	1.003(5)	0.054(13)
O(16)	0.504(7)	0.479(7)	0.287(6)	0.073(21)
O(18)	0.933(4)	0.858(3)	0.552(3)	0.019(8)
O(19)	0.265(3)	0.528(3)	0.479(3)	0.005(7)
O(21)	0.333	0.667	0.649(5)	0.019(14)

Atom	U_{11}	U_{22}	U_{33}	U_{23}	U_{13}	U_{12}
W(1)	0.017(2)	0.013(2)	0.042(3)	0.003(2)	0.001(2)	0.010(2)
W(2)	0.015(2)	0.015(2)	0.043(3)	0.003(2)	0.001(2)	0.009(2)
W(3)	0.017(2)	0.019(1)	0.024(2)	−0.009(2)	−0.004(1)	0.008(1)
Mg(1)	0.034(12)	0.043(13)	0.003(9)	−0.014(10)	0.000(9)	0.023(10)
Mg(2)	0.029(11)	0.038(14)	0.036(14)	0.001(12)	0.021(11)	0.012(11)
Mg(3)	0.038(12)	0.038(12)	0.000(15)	0.000	0.000	0.019(6)
Mg(4)	0.044(14)	0.044(14)	0.019(20)	0.000	0.000	0.022(7)
Si	0.029(10)	0.029(10)	0.038(20)	0.000	0.000	0.014(5)

[a] Standard deviations in the last significant digits are given in parentheses. The equivalent isotropic temperature factor is defined as one-third of the trace of the orthogonalized U tensor. For the oxygen atoms U_{eq} is equal to the isotropic temperature factor.

The overall geometry of unit (2) shows only small changes. The terminal oxygen atoms O(1) and O(2), which are bound only to W(1) and W(2), respectively, are now connected to Mg(2). Nevertheless, the W(1) and W(2) octahedra may be considered as type (I) octahedra. Both tungsten atoms are displaced from the centers towards the "pseudo" terminal oxygen atoms. This leads to the clearly shorter bond distances of 1.73(5) Å for W(1)–O(1) and 1.82(5) Å for W(2)–O(2) (see Table IV).

TABLE IV

BOND DISTANCES (Å) AND ANGLES (°) IN $Mg_8SiW_9O_{37} \cdot 12H_2O$ (COMPOUND B)

W(1) –O(1)	1.73(5)	O(1) –W(1)–O(8)	99(2)	O(9) –Mg(1)–O(8)	89(2)
W(1) –O(4)	1.85(4)	O(1) –W(1)–O(4)	99(2)	O(9) –Mg(1)–O(9)	85(3)
W(1) –O(8)	1.88(4)	O(1) –W(1)–O(3)	98(2)	O(9) –Mg(1)–O(6)	175(3)
W(1) –O(3)	1.95(3)	O(1) –W(1)–O(5)	96(2)		
W(1) –O(5)	2.06(4)	O(1) –W(1)–O(19)	169(2)	O(9) –Mg(1)–O(21)	76(2)
W(1) –O(19)	2.25(3)	O(8) –W(1)–O(4)	90(1)	O(9) –Mg(1)–O(16)	103(2)
		O(8) –W(1)–O(3)	86(2)	O(8) –Mg(1)–O(9)	173(3)
W(2) –O(2)	1.82(5)	O(8) –W(1)–O(5)	165(2)	O(8) –Mg(1)–O(6)	95(2)
W(2) –O(6)	1.89(5)	O(8) –W(1)–O(19)	90(2)	O(8) –Mg(1)–O(21)	100(2)
W(2) –O(4)	1.92(4)	O(4) –W(1)–O(3)	163(2)	O(8) –Mg(1)–O(16)	85(3)
W(2) –O(13)	2.00(4)	O(4) –W(1)–O(5)	90(2)	O(9) –Mg(1)–O(6)	91(2)
W(2) –O(3)	2.04(4)	O(4) –W(1)–O(19)	88(1)	O(9) –Mg(1)–O(21)	75(2)
W(2) –O(19)	2.25(4)	O(3) –W(1)–O(5)	90(2)	O(9) –Mg(1)–O(16)	99(2)
		O(3) –W(1)–O(19)	76(2)	O(6) –Mg(1)–O(21)	101(2)
W(3) –O(12)	1.61(5)	O(5) –W(1)–O(19)	75(1)	O(6) –Mg(1)–O(16)	81(3)
W(3) –O(5)	1.84(4)			O(21)–Mg(1)–O(16)	175(3)
W(3) –O(10)	1.87(3)	O(2) –W(2)–O(6)	97(2)		
W(3) –O(13)	1.88(5)	O(2) –W(2)–O(3)	99(3)	O(15)–Mg(2)–O(12)	121(3)
W(3) –O(10)	1.89(3)	O(2) –W(2)–O(4)	101(3)	O(15)–Mg(2)–O(15)	80(2)
W(3) –O(19)	2.51(3)	O(2) –W(2)–O(13)	98(3)	O(15)–Mg(2)–O(1)	85(2)
		O(2) –W(2)–O(19)	170(3)	O(15)–Mg(2)–O(2)	147(3)
Mg(1)–O(9)	1.99(4)	O(6) –W(2)–O(3)	87(2)	O(12)–Mg(2)–O(15)	118(3)
Mg(1)–O(9)	2.02(4)	O(6) –W(2)–O(4)	88(2)	O(12)–Mg(2)–O(1)	95(2)
Mg(1)–O(6)	2.03(5)	O(6) –W(2)–O(13)	164(2)	O(12)–Mg(2)–O(2)	92(2)
Mg(1)–O(16)	2.04(9)	O(6) –W(2)–O(19)	90(1)	O(15)–Mg(2)–O(1)	147(3)
Mg(1)–O(21)	2.04(4)	O(3) –W(2)–O(4)	161(1)	O(15)–Mg(2)–O(2)	88(3)
Mg(1)–O(8)	2.06(5)	O(3) –W(2)–O(13)	88(2)	O(1) –Mg(2)–O(2)	87(2)
		O(3) –W(2)–O(19)	75(1)		
Mg(2)–O(15)	1.98(8)	O(4) –W(2)–O(13)	91(1)	O(18)–Mg(3)–O(18)	88(2) 3×
Mg(2)–O(12)	2.09(5)	O(4) –W(2)–O(19)	87(1)	O(18)–Mg(3)–O(7)	171(3) 3×
Mg(2)–O(15)	2.12(9)	O(13)–W(2)–O(19)	75(2)	O(7) –Mg(3)–O(7)	100(3) 3×
Mg(2)–O(2)	2.15(7)			O(18)–Mg(3)–O(7)	87(2) 3×
Mg(2)–O(1)	2.21(6)	O(12)–W(3)–O(13)	101(3)	O(18)–Mg(3)–O(7)	85(2) 3×
		O(12)–W(3)–O(10)	108(3)		
Mg(3)–O(7)	1.93(7) 3×	O(12)–W(3)–O(5)	101(2)	O(9) –Mg(4)–O(9)	74(2) 3×
Mg(3)–O(18)	2.08(4) 3×	O(12)–W(3)–O(10)	107(2)	O(9) –Mg(4)–O(15)	104(2) 3×
		O(12)–W(3)–O(19)	169(2)	O(9) –Mg(4)–O(15)	102(3) 3×
Mg(4)–O(15)	2.06(6) 3×	O(13)–W(3)–O(10)	151(2)	O(15)–Mg(4)–O(9)	176(3) 3×
Mg(4)–O(9)	2.26(5) 3×	O(13)–W(3)–O(5)	89(2)	O(15)–Mg(4)–O(15)	80(3) 3×
		O(13)–W(3)–O(10)	90(2)		
Si –O(19)	1.66(3) 3×	O(13)–W(3)–O(19)	70(2)	O(19)–Si –O(19)	115(2) 3×
Si –O(21)	1.99(9)	O(10)–W(3)–O(5)	89(2)	O(21)–Si –O(19)	103(3) 3×
		O(10)–W(3)–O(10)	79(2)		
		O(10)–W(3)–O(19)	81(2)		
		O(5) –W(3)–O(10)	151(2)		
		O(5) –W(3)–O(19)	73(1)		
		O(10)–W(3)–O(19)	81(1)		

Whereas in compound A the W(3) atom shows a relatively regular environment, the $W(3)O_6$ octahedron in compound B is more distorted. This distortion is reflected by a very short W(3)–O(12) distance of 1.61(5) Å and the long W(3)–O(19) distance of 2.51(3)

TABLE V

CONNECTION SCHEME FOR $Mg_8SiW_9O_{37} \cdot 24.5H_2O$ (A) AND $Mg_8SiW_9O_{37} \cdot 12H_2O$ (B)[a]

	W(1)	W(2)	W(3)	Mg(1)	Mg(2)	Mg(3)	Mg(4)	Si
O(1)	+ ○				○			
O(2)		+ ○			○			
O(3)	+ ○	+ ○						
O(4)	+ ○	+ ○						
O(5)	+ ○		+ ○					
O(6)		+ ○		+ ○				
O(7)					2+	3+ 3○		
O(8)	+ ○			+ ○				
O(9)				2+ 2○			3+ 3○	
O(10)			2+ 2○					
O(11)					+			
O(12)			+ ○		○			
O(13)		+ ○	+ ○					
O(14)					+			
O(15)					2○		3+ 3○	
O(16)				+ ○				
O(17)					+			
O(18)						3+ 3○		
O(19)	+ ○	+ ○	+ ○					3+ 3○
O(20)					+			
O(21)				+ ○				+ ○

[a] The labelling of the metal and oxygen atoms was chosen in such a way that both structures are directly comparable. + indicates the connection for compound A and ○ for compound B. Differences occur only for Mg(2).

TABLE VI

OBSERVED W–W, W–O_A, W–O_B, AND W–O_C DISTANCES IN DIFFERENT POLYTUNGSTATES

	A	*B*	$W_6O_{19}^{2-}$ (*9*)	$H_2W_{12}O_{42}$ (*14*)
W–W				
From	3.341	3.339	3.281	3.327
To	3.398	3.411	3.296	3.373
Mean	3.379	3.384	3.286	3.351
W–O_A				
From	1.68	1.61	1.672	1.65
To	1.73	1.82	1.713	1.78
Mean	1.72	1.72	1.693	1.71
W–O_B				
From	1.77	1.84	1.892	1.78
To	2.09	2.06	1.948	2.17
Mean	1.92	1.92	1.924	1.94
W–O_C				
From	2.31	2.25	2.321	2.22
To	2.43	2.51	2.333	2.29
Mean	2.36	2.34	2.325	2.26

Å. It should be mentioned that the "terminal" oxygen atom O(12) is also bound to Mg(2). The bond lengths between W(3) and the four bridging atoms range from 1.84(4) to 1.89(3) Å. The mean values for W–O_A, W–O_B, and W–O_C are 1.72, 1.92, and 2.34 Å, respectively. These mean distances are within the range observed in other compounds and nearly the same as in compound A (see Table VI for comparison).

Applying bond length–bond strength correlations to these mean bond distances we estimate $s_{mean} = 1.84$ for W–O_A, 0.95 for W–O_B, and 0.29 for W–O_C. There are no significant differences in the s_{mean} values compared to those of compound A. Without going into more detail, the O_A–W–O_B and O_B–W–O_B angles in the W(1) and W(2) octahedra are only slightly different from those in compound A (Table VII). As can be deduced from angles and distances (see Tables IV and VII), the Mg(1) and Mg(4)

TABLE VII

COMPARISON OF ANGLES AROUND THE DIFFERENT METAL ATOMS IN COMPOUNDS A AND B (°)

O_A–W(1)–O_B	91(1)–104(1)	96(2)–99(2)
O_B–W(1)–O_B	83(1)–165(1)	86(2)–165(2)
O_A–W(1)–O_C	165(1)	169(2)
O_B–W(1)–O_C	74(1)–89(1)	75(1)–90(2)
O_A–W(2)–O_B	93(1)–102(1)	97(3)–101(3)
O_B–W(2)–O_B	84(1)–164(1)	87(1)–164(2)
O_A–W(2)–O_C	166(1)	170(2)
O_B–W(2)–O_C	74(1)–90(1)	75(1)–90(1)
O_A–W(3)–O_B	99(1)–101(1)	101(3)–108(3)
O_B–W(3)–O_B	86(1)–160(1)	79(2)–151(2)
O_A–W(3)–O_C	173(1)	169(2)
O_B–W(3)–O_C	75(1)–84(1)	70(2)–81(2)
O–Mg(1)–O neighbored	86(1)–95(1)	75(2)–103(2)
opposite	175(1)–178(1)	173(3)–176(3)
O–Mg(2)–O neighbored	83(1)–99(1)	80(2)–95(2)
opposite	175(1)–177(1)	118(3)–147(3)
O–Mg(3)–O neighbored	82(1)–92(1)	85(2)–100(3)
opposite	172(1)	171(3)
O–Mg(4)–O neighbored	82(1)–99(1)	74(2)–104(3)
opposite	174(1)	176(3)
O–Si–O	107(1)–112(1)	103(3)–115(2)

environments are more distorted compared with those of compound A. The Si tetrahedron is less regular with one longer and three distinctly shorter Si–O bonds.

Further Thermal Dehydration

The thermogravimetric curve (Fig. 2) shows that further dehydration of compound B occurs in two steps, the first of which is relatively well defined (weight loss 2.8%) between 210 and 300°C, followed by a more or less continuous weight loss of 1.4% up to 470°C. At this temperature, when all the water has been driven off, an exothermic peak in the DTA curve appears, indicating a possible phase transformation. These observations are explained by the continuous high-temperature X-ray diffractogram (Fig. 3). The dehydration of compound B leads to an X-ray amorphous hydrated phase, which dehydrates only slowly. As all the water is lost, crystallization occurs into a poorly crystalline phase, the X-ray powder diffraction of which corresponds closely to that published for a high-temperature form of $MgWO_4$ (*13*) stable above about 1200°C. This rather unusual finding is, however, the same as in the dehydration of $MgWO_4 \cdot 2H_2O$ (*3*), where this same "high-temperature modification" has been found to appear before the stable wolframite-type structure on dehydration. Indeed, it is transformed into the wolframite type at temperatures around 650°C. There are indications in the literature that this observation has in fact been made by most earlier authors who have studied the formation of $MgWO_4$ from hydrated precursors, but it has never been clearly stated. This has been discussed already in (*3*). The most significant difference in the dehydration of $MgWO_4 \cdot 2H_2O$ and the compounds treated in this paper is the appearance of an amorphous intermediate in the present case.

Summary and Discussion

The trigonal magnesium heteropolytungstates exhibit a number of peculiar features, both in their crystal structures and in their dehydration behavior. They represent to our knowledge the first heteropoly metalates containing magnesium. It is therefore not surprising that their crystal structures contain building units not described so far. In compound A ($Mg_8SiW_9O_{37} \cdot 24.5H_2O$) two such units are clearly identified: unit (1), which might also be described as an isopoly magnesium salt, consists of four edge-sharing octahedra with the overall composition (Mg_4O_{16}) (because the hydrogens have not been located, no charge can be assigned to this formula), resembling an isolated domain of the MgO lattice. On the other hand, unit (2) may be described either by addition of three groups of three edge-sharing tungsten coordination octahedra each to unit (1), or as a derivative of the Keggin ion structure by replacing three tungsten atoms by magnesium and adding a further magnesium coordination octahedron to it. It also contains a silicon atom in the central tetrahedral interstice. Its overall composition corresponds to $Mg_4SiW_9O_{43}$. In between these two units, uncoordinated water is situated on an incompletely occupied crystallographic position.

Whereas in the very first step of dehydration only interstitial water is lost, the second step leading to compound B ($Mg_8SiW_9O_{37} \cdot 12H_2O$) changes the structure more profoundly. Unit (1) is destroyed by displacement of three of its metal atoms towards unit (2), leaving an isolated MgO_6 octahedron as a new structural element. The addition of the three displaced magnesium atoms to unit (2) occurs in such a way as to place them in a very unusual five-coordinated rectangular pyramidal position, thus connecting the formerly isolated units (2) to a three-dimensional network. A striking property of these compounds is that their

interconversion is highly topotactic and fully reversible, producing pseudomorphous product particles which can be treated almost as single crystals and are of sufficient quality for an X-ray diffraction structure determination. In twenty years of occupation with topotactic reactions, we have never observed such a high degree of topotaxy in a dehydration/rehydration process.

Further heating, however, apparently causes the three-dimensional network to collapse completely, leading to an X-ray amorphous hydrated intermediate. After complete removal of water, it crystallizes into a phase described earlier as the high-temperature form of $MgWO_4$ stable only above ca. 1200°C (*13*), but is transformed into the stable low-temperature form of the wolframite type in an exothermic transition at 470°C. This unusual behavior can be attributed to the topochemical character of the process and corresponds to Ostwald's rule of successive phase transformations. A similar process, but without the appearance of an amorphous intermediate, has been observed in the dehydration of $MgWO_4 \cdot 2H_2O$, and there are indications in the earlier literature that in fact "high-temperature $MgWO_4$" is formed first in processes leading to anhydrous $MgWO_4$ from hydrated precursors, as discussed in (*3*).

Acknowledgments

We thank Dr. R. Prewo for letting us use the Syntex P21 diffractometer, Dr. V. Gramlich for helpful discussions, and Dr. J. Sommerauer for the microbeam analysis. Financial support from the Swiss National Science Foundation (Project 2.023-0.83) is gratefully acknowledged.

References

1. N. J. DUNNING AND H. D. MEGAW, *Trans. Faraday Soc.* **42,** 705 (1946).
2. J. R. GÜNTER, "Reactivity of Solids," Proceedings, 10th ISRS, Dijon, 1984, Elsevier, Amsterdam; *Mater. Sci. Monogr. A* **28,** 485 (1985).
3. J. R. GÜNTER AND E. DUBLER, *J. Solid State Chem.* **65,** 118 (1986).
4. G. M. SHELDRICK, "SHELXS-84, Crystal Structure Solution," University of Göttingen, 1984.
5. W. C. HAMILTON, *Acta Crystallogr.* **18,** 502 (1965).
6. E. DUBLER, G. B. JAMESON, AND Z. KOPAJTIC, *J. Inorg. Biochem.* **26,** 1 (1986).
7. M. T. POPE, "Heteropoly and Isopoly Oxometalates," Inorganic Chemistry Concepts, Vol. 8, Springer-Verlag, Berlin/Heidelberg/New York/Tokyo (1983).
8. M. T. POPE, *Inorg. Chem.* **11,** 1973 (1972).
9. J. FUCHS, W. FREIWALD, AND H. HARTL, *Acta Crystallogr., Sect. B* **34,** 1764 (1978).
10. R. STOMBERG, *Acta Chem. Scand., Ser. A* **39,** 507 (1985).
11. G. M. SHELDRICK, "SHELX-76, Program for Crystal Structure Determination," University of Cambridge, 1976.
12. "International Tables for X-Ray Crystallography," Vol. III, Kynoch Press, Birmingham, UK (1965).
13. L. L. Y. CHANG, M. G. SCROGER, AND B. PHILLIPS, *J. Amer. Ceram. Soc.* **49,** 385 (1966).
14. H. D'AMOUR AND R. ALLMANN, *Z. Kristallogr.* **138,** 5 (1973).
15. R. X. FISCHER, STRUPLO, *J. Appl. Crystallogr.* **18,** 258 (1985).
16. I. D. BROWN AND K. K. WU, *Acta Crystallogr., Sect. B* **32,** 1957 (1976).